JOURNAL OF MATERIALS SCIENCE **37** (2002) 3569–3572

Effect of heating conditions during combustion synthesis on the characteristics of $Ni_{0.5}Zn_{0.5}Fe_2O_4$ nanopowders

A. C. F. M. COSTA
Department of Materials Eng., Federal University of Paraíba, 58970-000, Campina Grande, Brazil

E. TORTELLA, M. R. MORELLI
Department of Materials Eng., Federal University of São Carlos, 13.565-905, São Carlos, Brazil

M. KAUFMAN
Department of Materials Science Eng., University of Florida, Florida, USA

R. H. G. A. KIMINAMI
Department of Materials Eng., Federal University of São Carlos, 13.565-905, São Carlos, Brazil
E-mail: ruth@power.ufscar.br

Ni-Zn ferrite powders were synthesized by combustion reaction. The effect of external conditions of heating on the characteristics of the resulting powders was evaluated. Two synthesis routes were studied. The first involved preheating on a hot plate at 300°C and subsequently heating in a muffle furnace at 700°C (RCPM). In the second route the powders (RCP) were heated directly to 600°C on a hot plate until self-ignition occurred. The resulting RCP products were evaluated before and after attritor milling in order to reduce the size and increase the uniformity of particles and/or agglomerates. The resulting powders were characterized by X-ray diffraction (XRD), BET, scanning electron microscopy (SEM), helium pycnometry, sedimentation and transmission electron microscopy (TEM). The results showed that it was possible to obtain Ni-Zn ferrite powders using both routes and that the second route (RCP) was the most favorable in terms of obtaining powders with high surface area. The efficiency of the grinding was confirmed by the reduction of the size of the particles.

1. Introduction

In recent years, a considerable amount of research has been carried out on Ni-Zn ferrites because of their innumerable applications in non-resonant devices, radio frequency circuits, high-quality filters, rod antennas, transformer cores, read/write heads for high-speed digital tapes and operating devices [1–3].

Wide ranges of chemical methods have recently been used to obtain Ni-Zn ferrite powders. Among the current preparation methods, combustion synthesis stands out as an alternative and highly promising technique for the preparation of these materials [4]. The process is quite simple since multiple steps are not involved. It is employed in the field of propellants and explosives, and involves an exothermic and self-sustaining chemical reaction between the desired metal salts and a suitable organic fuel, usually urea [4, 5]. The resulting product is usually a product that is dry, crystalline, has high chemical homogeneity and purity, is inexpensive, and is agglomerated into a highly fluffy foam [6, 7]. The heating conditions affect the characteristics of the resulting powders. According Zhang [6], a key feature of the combustion process is that the heat required to sustain the chemical reaction is provided by the reaction itself and not by an external source. The results of many publications on powder synthesis by combustion reaction has shown that several different heating methods hot-plate [8, 9], hot-plate and muffle [9–14], or muffle-furnace only [15–17] for the initiation of the combustion reaction may be used, but it has not been discussed whether these different methods provide powders with similar or different compositions and/or characteristics. In this paper, we report the preparation of Ni-Zn ferrite powders by combustion reactions using two different heat sources for the combustion process.

2. Experimental methods

The materials used were iron nitrate [$Fe(NO_3)_3 \cdot 9H_2O$], zinc nitrate [$Zn(NO_3)_2 \cdot 6H_2O$], nickel nitrate [$Ni(NO_3)_2 \cdot 6H_2O$] and urea [$CO(NH_2)_2$]. Stoichiometric composition of the metal nitrate and urea were

calculated using the total oxidizing and reducing valences of the components which serve as the numerical coefficients for the stoichiometric balance, so that the equivalence ratio, Φ_c, is unity and the energy released is a maximum [5]. Two different external heating methods were studied: in the first, the solution was pre-heated a hot plate to around 300°C and then transferred to a muffle-furnace at 700°C until ignition occurred (RCPM). In the second approach, the solution was directly heated on the hot plate to around 600°C until ignition happens (RCP). The reaction products obtained by RCP were ground for 20 min in an attritor mill (Szegvari Attritor System, Type, 01STD, Union Process) and named RCPA. The reaction temperature was determined by an infrared pyrometer (Raytek, model MA2SC). All powders were characterized by X-ray diffraction (Kristaloflex D5000, Cukα with a Ni filter). The average crystallite sizes were calculated from X-ray line broadening using the 311 peaks and Scherrer's equation [18]. A sedimentation (HORIBA-Particle Size Distribution Analyzer, CAPA-700 U.S. version) apparatus was used to measure the particle size distribution and a BET (Quantasorb Quantachrome model Gemini-2370 Micromeritics) to measure the specific surface area by the physical adsorption of N_2 gas at cryogenic temperature. The density was determined using a helium pycnometer (Pycnometer Micromeritics, ACCUPYC 1330) and the morphology, size of the particles by scanning electron microscopy (Carl Zeiss 940A) and transmission electron microscopy (TEM). For the TEM studies samples were supported on carbon-coated copper TEM grids and analyzed using a Philips EM420 transmission electron microscope at an accelerating voltage of 120 kV. Bright-field and dark-field imaging was performed to reveal the size and morphology of the nanopowders. Structure information was obtained using selected area diffraction.

3. Results

The ignition temperatures of the two heating methods (RCPM and RCP) were determined using the infrared pyrometer to be 966°C (±2°C) and 703°C (±2°C), respectively. The external conditions (hot plate vs. hot-plate plus muffle furnace) changed the kinetics and the exothermic nature of the reaction specifically. The combustion reactions by RCPM were slower than those by RCP and these differences are attributed to the different atmosphere conditions in the muffle furnace (low oxygen) compared with those on the hot plate (normally atmospheric conditions). The reaction on direct heating on the hot plate to temperatures around 600°C was very quick and reached 703°C. This difference in the atmosphere and ignition temperature leads to the formation of powders with different characteristics. Table I shows the characteristics of these powders obtained by combustion reactions for the routes previously discussed (RCP and RCPM). Through picnometry results one can observe that the density of the two powders was about 97.2 and 99.9% of the theoretical density. The average agglomerate size, specific superficial area (BET) and size of the nanoparticles calculated starting from BET

TABLE I Characteristics of powders prepared by combustion reaction

Composition ($Ni_{0.5}Zn_{0.5}Fe_2O_4$)	RCPM	RCP	RCPA
Specific surface area (BET) (m^2/g)	6.1	38.9	44.3
Average agglomerate size[a] 50%[a] (μm)	11.0	3.8	3.2
Particle size[b] (nm)	190	29	26
Particle size[c] (nm)	79	39	29
Powder density (g/cm^3) (% of theoretical density)	5.21 (99.9)	5.11 (97.2)	5.05 (96.1)

[a]Particle agglomerates.
[b]From specific surface area.
[c]From Scherrer's equation.

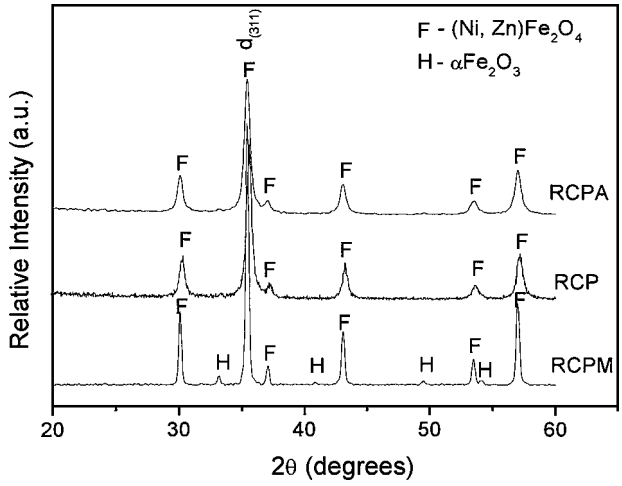

Figure 1 X-ray powder diffraction patterns of powders prepared by combustion synthesis.

were 3.8–11.0 μm, 38.9–6.1 m^2/g and 29–190 nm, respectively. It can be observed that the resulting powder from RCP presented a specific superficial area value that was six-fold that obtained by RCPM. This fact indicates that normal atmosphere and ignition temperature control yielded powders with greater specific surface area. The characteristics of the samples (RCPA) milled for 20 min in the attritor mill showed little difference in size of the particles, from the samples prior to milling.

Fig. 1 shows the X-ray patterns of the resulting powders from RCPM, RCP and RCPA. The powders prepared by the RCPM route revealed a small amount of hematite (α-Fe_2O_3) as a secondary phase and Ni-Zn ferrite as the major phase. However, the powders resulting from the RCP route appeared to contain only single-phase crystalline Ni-Zn ferrite. These results show the strong influence of the atmosphere on the formation of the Ni-Zn ferrite phase. The presence of the hematite phase detected in the sample from the RCPM route can be attributed to the smaller oxygen content inside the muffle necessary for complete crystallization.

The XRD patterns of the RCP powder showed considerable line broadening indicating the nanoparticle nature in contrast to the smaller line broadening observed for large RCPM powders. The crystallite sizes calculated from X-ray line (d_{311}) broadening using Scherrer's equation [10] were 79 and 39 nm for the

powders prepared by RCPM and RCP, respectively. These results are in agreement with those calculated from the specific superficial area for the powders obtained by the two routes. Crystallite sizes calculated from specific surface area and Scherrer's equation for the RCPM powders were 79 nm and 190 nm, respectively, consistent with the large mean size of the RCPM distributions for this powder. For the resulting powders from RCPA, the crystallite size determined by Scherrer's equation approximated to the average particle size calculated from specific surface area, and approximated to the results obtained without the additional grinding process.

Fig. 2 shows the morphology of the resulting powders synthesized by RCPM and RCP indicating that the nanoparticles tended to be agglomerated. A sharp reduction in agglomerate size was observed for the RCP powder (Fig. 2b), for which the combustion reaction was quicker than for the RCPM route. The agglomerate size determined from the micrographs were 38.97 ± 31.61 and 6.82 ± 5.77 μm for the two powders, respectively.

For the TEM studies, bright field (BF) and centered dark field (CDF) images along with selected area diffraction patterns (SADPs) were obtained from the agglomerated clusters of powders. For the CDF images, the objective aperture was sufficiently large to contain the strongest two inner rings (311 and 200). For the SADPs, the selected area aperture size was kept constant as was the area covered by the aperture in the image. This allowed us to obtain a better indication of the crystal size (CDF) vs. the actual powder size (BF) in the powders since they should be different if the individual powders are polycrystalline.

Fig. 3 shows the size and morphology of as-synthesized Ni-Zn ferrites particles observed by TEM micrograph. The powders appeared to be agglomerated. The electron diffraction pattern clearly shows in both cases rings belonging to the Ni-Zn ferrite phase and also rings corresponding to spacing of around 2.97 Å and 1.62 Å of the Ni-Zn ferrite. The selected area aperture used in this study was enough to reveal all the

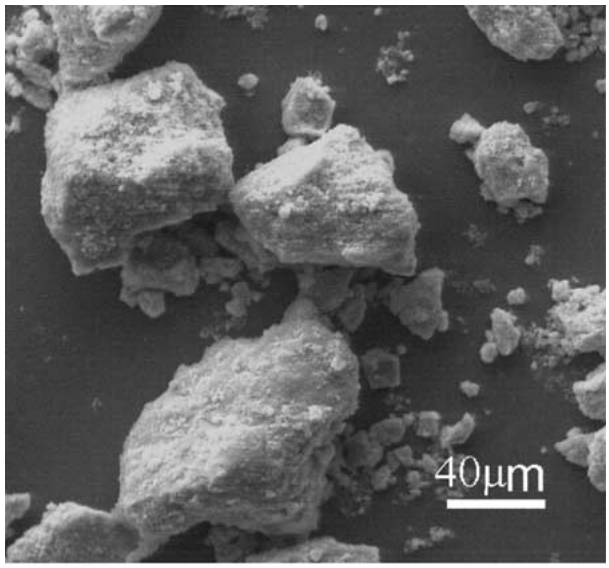

(a)

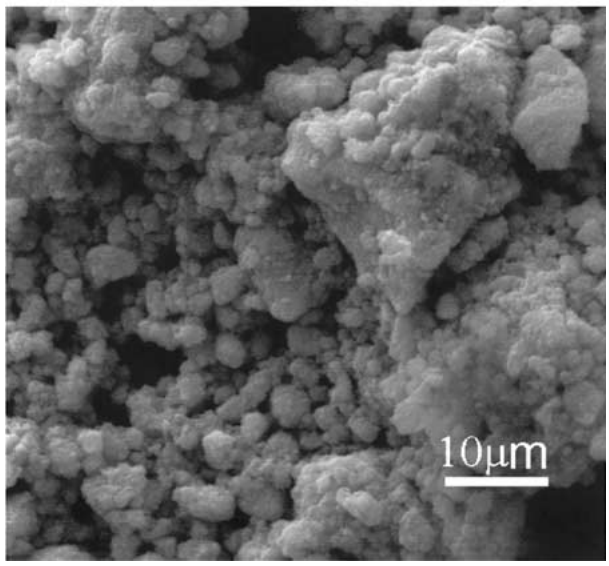

(b)

Figure 2 Morphology of the powders synthesized by combustion reaction using the two different heating methods. (a) hot-plate and muffle furnace (RCPM) and (b) hot-plate only (RCP).

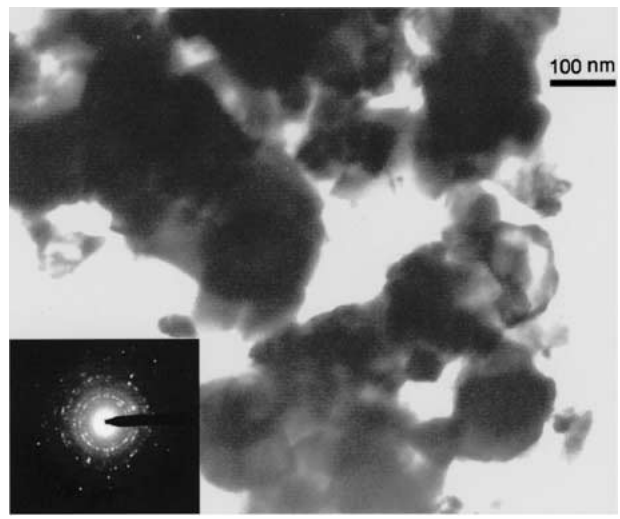

(a)

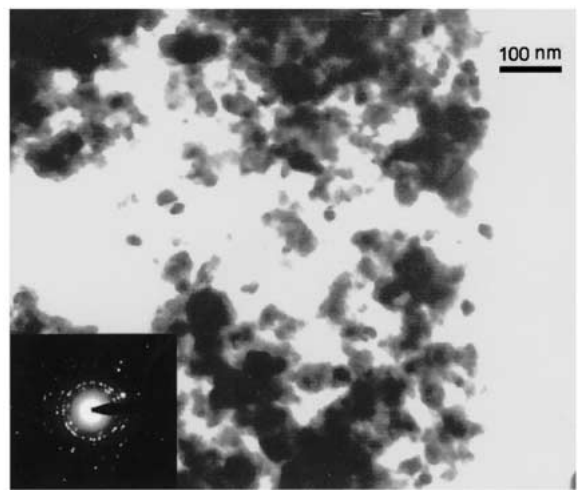

(b)

Figure 3 TEM micrographs of the powders synthesized by combustion reaction with to different heating conditions (a) muffle and plate (RCPM) and (b) plate (RCP).

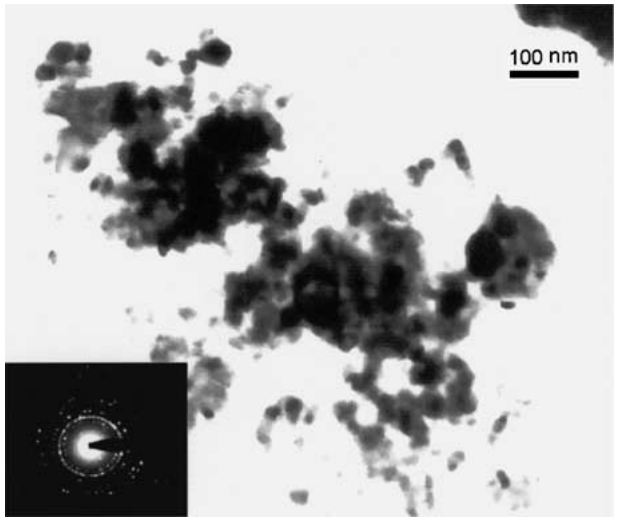

Figure 4 TEM micrographs of the powders synthesized by plate heating condition and milled for 2 h (RCPA).

correspondent rings for the spinel structure. The TEM results showed that the particles did not have a narrow size distribution. Thus it can be inferred that nucleation occurred as a single event, and this resulted in a size distribution of nuclei. The particle sizes from TEM micrographs were in the range of 11–30 nm and 60–97 nm for the RCP and RCPM powders. These results are in good agreement with the results obtained by BET and Scherrer's equation (Table I).

As seen in Fig. 4, the RCP and RCPA powder particles were similar in size (11–30 nm in diameter) and distribution. The RCPM powders appeared considerably coarser (60–90 nm in diameter), as is evident in both the BF/CDF images as well as in the less continuous distribution in the rings in the SADPS from these powders.

These results show how important are the external conditions that initiate ignition and sustain the chemical reaction in adequate atmosphere conditions. Different external conditions of heating lead to different nanopowder characteristics.

4. Conclusions

The results obtained in this study demonstrate that the external heating conditions used to initiate and sustain the combustion reaction in the synthesis of Ni-Zn ferrite affect the characteristics of the resulting powders. The combustion reaction realized in the plate and muffle (RCPM) was strongly affected by the atmospheric conditions (low pressure oxygen) necessary to complete the reaction and crystallization of the Ni-Zn ferrite phase. This powder contained some second phase hematite and had average particle size 70–190 nm.

The reaction accomplished directly on the heating plate (RCP) resulted in Ni-Zn ferrite powders with excellent nano-characteristics, particles sizes between 15–30 nm and surface areas of 38.9 m^2/g. The subsequent stage of grinding in the attritor (RCPA) caused no significant increase in the nano-characteristics of these Ni-Zn ferrites. The combustion synthesis was sufficient to obtain Ni-Zn ferrite nano-particles, without subsequent milling.

Acknowledgements

We would like to thank the Brazilian institutions, FAPESP, CNPq and CAPES for financial support.

References

1. P. RAVINDERNATHAN and K. C. PATIL, *J. Mater. Sci.* **22** (1987) 3261.
2. H. IGARASH and K. OHAZAKI, *J. Amer. Ceram. Soc.* **60** (1997) 51.
3. A. GOLDMAN, *Am. Ceram. Soc. Bull.* **63** (1984) 582.
4. R. H. G. A. KIMINAMI and J. KONA, *Powder and Particle* **19** (2001) 156.
5. S. R. JAIN, K. C. ADIGA and V. PAI VERNEKER, *Combust. Flame* **40** (1981) 71.
6. Y. ZHANG and G. C. STANGLE, *J. Mater. Res.* **9**(8) (1994) 1997.
7. S. T. ARUNA and K. C. PATIL, *J. Mater. Syn. Proc.* **4**(3) (1996) 175.
8. D. A. FUMO, M. R. MORELLI and A. M. SEGADÃES, *Mater. Res. Bull* **31** (1996) 1243.
9. S. S. MANOHARAN and K. C. PATIL, *J. Amer. Ceram. Soc.* **75** (1992) 1012.
10. J. J. KINGSLEY and K. C. PATIL, *Mater. Lett.* **6** (1988) 427.
11. E. BREVAL and D. K. AGRAVAL, *J. Amer. Ceram. Soc.* **81** (1998) 1729.
12. A. M. SEGADÃES, M. R. MORELLI and R. H. G. A. KIMINAMI, *J. Eur. Ceram. Soc.* **18** (1998) 771.
13. V. C. SOUSA, Thesis, Federal University of São Carlos. São Carlos (2000).
14. R. H. G. A. KIMINAMI, M. R. MORELLI, D. FOLZ and D. E. CLARK, *Mater. Trans.* **42**(8) (2001) 3601.
15. D. A. FUMO, J. R. JURADO, A. M. SEGADÃES and J. R. FRADE, *Mater. Res. Bull.* **32** (1997) 1459.
16. T. SATO, F. OZAWA and S. IKOMA, *Appl. Chem. Biotechno.* **28** (1978) 811.
17. S. BHADURI, E. ZHOU and S. B. BHADURI, *Ceram. Eng. & Sci.* **18** (1997) 645.
18. H. KLUNG and L. ALEXANDER, in "X-ray Diffiraction Procedures" (Wiley, New York, EUA., 1962) p. 491.

Received 5 December 2001
and accepted 30 April 2002